

# The statistics of accelerations seen in radial velocity searches for planets

Alice C. Quillen

*Department of Physics and Astronomy, University of Rochester, Rochester, NY 14627*

21 February 2019

## ABSTRACT

Radial velocity searches for extrasolar planets have discovered stars undergoing slow accelerations. The accelerations are likely due to one or more gas giant planets or brown dwarfs orbiting with period longer than the total time span of observations. The stellar acceleration is proportional to the mass of the companion divided by the square of its radius from the star. In this paper we predict the distribution of accelerations using a Monte Carlo method and assuming a semi-major axis and mass distribution for the companions. Radial velocity surveys find that  $\sim 20$  and  $10\%$  of stars surveyed exhibit accelerations above  $\sim 10$  and  $25 \text{ m s}^{-1} \text{ yr}^{-1}$ , respectively. We find that an extrapolation of the size and period distribution found by radial velocity surveys within  $\sim 5$  AU or companion imaging surveys predicts too few systems with detectable accelerations. The fractions of stars with accelerations above these values can be matched if every star hosts a gas giant planet or brown dwarf with semi-major axes between 4 and 20 AU or if a significant fraction ( $\sim 70\%$ ) of stars host 3 or more massive planets in this range. This suggests that there is a large undiscovered population of gas giant planets and brown dwarfs present with semi-major axes in the 5–30 AU range.

## 1 INTRODUCTION

Radial velocity searches for extrasolar planets often find linear trends in the observed velocity of a star (Butler et al. 2006; Wittenmyer et al. 2006; Wright et al. 2007; Patel et al. 2007; Marcy et al. 2008). These correspond to velocity variations or constant accelerations of the star by massive objects in the system. As the time span of observations increases these accelerations begin to vary (e.g., Wright et al. 2007; Patel et al. 2007), then finally a substantial fraction of the an orbital period becomes recognizable as the entire Keplerian velocity curve is recognized. Trends or accelerations have been seen in radial velocity surveys (Butler et al. 2006) and used to place limits on mass and radii of long period planets residing in the system (Wittenmyer et al. 2006, 2007; Wright et al. 2007). Planets are not considered detected by radial velocity or transit surveys until at least a full orbital period is seen (O’Toole et al. 2008). This is justifiable as it is difficult, perhaps impossible when noise is present, to constrain simultaneously planet mass, semi-major axis and orbital eccentricity from radial velocity observations alone over only a fraction of a period (Brown 2004; Wright et al. 2007), but see the study by Patel et al. (2007). Once an entire period is observed, the period of the orbit sets the planet’s semi-major axis. As the amplitude of the radial velocity perturbation depends on both the mass and period, once the period is known, the mass of the planet can be estimated. Because only poor constraints on both planet and semi-major axis can be made

from constant or slowly changing accelerations, radial velocity surveys place only poor constraints on exoplanets at large semi-major axis where the orbital periods are long.

In the next decade we have the prospect of both more sensitive radial velocity surveys (nearing  $1 \text{ m/s}$  in precision) and multi-object radial velocity surveys. These surveys will increasingly find stars with measured accelerations that don’t correspond to complete orbital periods. In this paper we consider the distribution of these trends and how they can be used to constrain the mass and semi-major axis distribution of massive objects in outer exo-planetary systems even though the exact masses and semi-major axes are not directly measured. By outer we mean above 5 AU. The orbital period at 5 AU around a solar mass star is about 11 years, corresponding to the lifespan of a decade length multi-object radial velocity survey. This semi-major axis is within the limit of most current direct planet detection methods. However the statistics of objects inferred from the statistics of radial velocity trends will be complimentary to and motivate direct detection surveys searching for brown dwarfs and planets at wider separations (e.g., Metchev & Hillenbrand 2008; Kraus et al. 2008) and transit surveys that primarily find planets within an AU of their host star.

## 2 THE ACCELERATION OF A STAR CAUSED BY A LOW MASS COMPANION

We first consider the acceleration of a star caused by a single planet or brown dwarf in orbit. In the center of mass frame of 2 gravitationally bound bodies with masses  $m_1$  and  $m_2$  at positions  $\vec{x}_1$  and  $\vec{x}_2$ , the position of the more massive body is

$$\vec{x}_1 = \frac{m_2}{M}(\vec{x}_1 - \vec{x}_2) = \mu\vec{r} \quad (1)$$

where  $M = m_1 + m_2$  is the sum of the masses of the two bodies, the mass ratio  $\mu = m_2/M$  and the vector between the two bodies  $\vec{r} = \vec{x}_1 - \vec{x}_2$ . The acceleration of the more massive body or host star

$$\ddot{\vec{x}}_1 = \mu\ddot{\vec{r}}. \quad (2)$$

For the two body Kepler problem

$$\ddot{\vec{r}} = -\frac{GM\hat{r}}{r^2} \quad (3)$$

where  $G$  is the gravitational constant and  $\hat{r}$  is the unit vector between the two masses. Combining the previous two equations we find that the acceleration of the central star

$$\ddot{\vec{x}}_1 = -\frac{\mu GM\hat{r}}{r^2}. \quad (4)$$

The acceleration toward the viewer measured from changes in the radial velocity is  $a_r = \ddot{\vec{x}}_1 \cdot \hat{e}_{los}$  where  $\hat{e}_{los}$  is the unit vector pointing toward the observer. In physical units

$$a_r = 187 \text{ m s}^{-1} \text{ yr}^{-1} \left( \frac{r}{\text{AU}} \right)^{-2} \left( \frac{\mu}{10^{-3}} \right) \left( \frac{M}{M_\odot} \right) \hat{r} \cdot \hat{e}_{los}. \quad (5)$$

We note that the magnitude of the acceleration depends on  $\mu M/r^2 = M_p/r^2$ , where  $M_p$  is the mass of the planet and is independent of the stellar mass. We expect the distribution of accelerations to depend on the ratio of the companion mass divided by the square its semi-major axis. This dependence is reflected in the upper limit plots (mass vs period) by Wittenmyer et al. (2006) (see their Figure 4) derived from trends (accelerations) seen with the McDonald Observatory planet search program. For comparison the amplitude of the radial velocity variation during an entire orbit is proportional to  $\mu\sqrt{M/a}$  (e.g., equation 1 Cumming et al. 2008). We expect the statistics of accelerations to differ from those of radial velocity amplitudes.

The distribution of extrasolar planets discovered in radial velocity surveys is consistent with  $dN/d\log a \propto a^{0.4}$  (Marcy et al. 2008) implying that there is increasing numbers of giant planets at larger semi-major axes. For a semi-major axis greater than 10 AU, where an entire orbital period would not be detected in a moderate time span radial velocity survey, equation 5 predicts an acceleration of  $1.9 \text{ m s}^{-1} \text{ yr}^{-1} (M_p/M_J)$  which is near the detection limit of radial velocity surveys. Here  $M_J$  is the mass of Jupiter. However companion masses in the brown dwarf range (between 13 and 80  $M_J$ , Burrows et al. 1997) at semi-major axes between 10 and 100 AU can cause accelerations detectable in radial velocity surveys. Hence accelerations measured from radial velocity surveys are sensitive to massive planets and brown dwarfs in the outer regions of extrasolar systems. This range of masses contains brown dwarfs and so the region identified as the brown dwarf desert where there is a deficit of known objects (Grether & Lineweaver 2006).

Previous studies have recognized that incomplete orbits detected in radial velocity studies are most likely caused by companion brown dwarfs (Patel et al. 2007).

Cumming et al. (2008) found that  $\sim 23\%$  of the total stars surveyed showed a significant slope or velocity variations (corresponding to accelerations) across 8 years of observations. The mean error of their survey was less than 3 m/s so the velocity variations detected would be similar to accelerations (along line of sight) are above few  $\text{m s}^{-1} \text{ yr}^{-1}$ . With less precision Nidever et al. (2002) found that 12% of the stars surveyed varied by more than above 100  $\text{m s}^{-1}$  across 4 years, corresponding to accelerations above 25  $\text{m s}^{-1} \text{ yr}^{-1}$ . A period of 4 years corresponds to a semi-major axis of 2.5 AU. If we restrict the semi-major axis to greater than 3 AU and use Equation 5, the level of accelerations seen by Nidever et al. (2002) requires planet masses above 1  $M_J$  if they are found at semi-major axes above 3 AU. We have conservatively chosen a semi-major axis corresponding to a period only slightly longer than the survey length. As the acceleration switches sign every half period it likely the objects responsible for these accelerations are at semi-major axis with periods larger than twice the survey length. For the longer Keck planet search 8 years corresponds to a semi-major axis of 4 AU. If we restrict the companion semi-major axis to 6 AU then again a planet mass above 1  $M_J$  is required to account for the observed velocity variations. The large fractions of objects exhibiting detected accelerations suggests that there is significant population of massive objects in the outskirts of exo-planetary systems. This is consistent with the extrapolation to larger semi-major axes discussed by Cumming et al. (2008) who estimated the number of systems with planets based on size distribution of inner planets exhibiting full periods during the span of observation.

## 3 MONTE CARLO SIMULATIONS

To compare the number of objects with accelerations to those predicted from the size and period distributions we use a Monte Carlo method (similar to the study by Brown 2004). We compute the line of sight component of the acceleration  $a_r$ , based on a distribution of systems with planets. We first consider the distribution of accelerations that would be seen from a very simple population. We consider a group of systems, each with one massive planet or brown dwarf companion at random positions in their orbits and at random inclinations. Mean anomalies and arguments of perihelia are randomly chosen from a flat probability distribution. Eccentricities are chosen from a flat eccentricity distribution with minimum and maximum eccentricities  $e_{min}$  and  $e_{max}$ . Orbital inclinations are chosen by generating  $\cos i$  with a flat probability distribution between -1 and 1 (Brown 2004, equation 17). After randomly generating orbital elements the Cartesian coordinates of each system are computed using Kepler's equation. Then the coordinates of the system are projected into viewer coordinates using the randomly selected system inclination. Equation 5 is used to predict the line of sight component of the acceleration. Acceleration distributions are computed using  $10^5$  sample star systems.

Figure 1 shows the distribution of the radial or line of sight component of acceleration  $a_r$  computed for a popula-

tion of systems with  $10 M_J$  bodies at 5 and 10 AU chosen with flat eccentricity distributions. For each semi-major axis, we show eccentricity distributions that consist of objects in circular orbits, range from 0 to 0.5 or 0 to 0.99. As planets on high eccentricity orbits have higher accelerations when they approach the star, the acceleration distributions extend to higher velocities when the eccentricity distribution is wider.

For these simple systems we ask what is the fraction of objects that would be observed with accelerations greater than a particular value, 5, 10 or  $25 \text{ m s}^{-1} \text{ yr}^{-1}$ ,  $f_5$ ,  $f_{10}$  and  $f_{25}$ . These fractions mimic the fraction of objects with trends reported by Cumming et al. (2008); Nidever et al. (2002). These fractions are listed in Table 1 and are measured from the same simulations that made the acceleration distributions shown in Figure 1.

The fraction of stars,  $f_5$ ,  $f_{10}$  and  $f_{25}$ , with accelerations above 5, 10 or  $25 \text{ m s}^{-1} \text{ yr}^{-1}$  is not high. The fraction  $f_{25}$  does not approach the 12% based on the survey by Nidever et al. (2002) except for the systems with masses above  $5 M_J$  mass planets at small radii at or below 5 AU. The fractions  $f_5$  or  $f_{10}$  do not approach the 23% estimated (based on the report by Cumming et al. 2008) unless masses are above  $5 M_J$ . The fractions shown in Table 1 were computed assuming that every system contains a single massive planet. The fraction of stars showing accelerations is necessarily lower than the fraction of systems with planets (here assumed to be all systems) as some of the systems are viewed face on and systems are viewed at different times in their orbit. The larger fraction of stars with accelerations compared to those predicted with this simple model suggests that one massive object is required at 5-20AU in almost all systems or more than one massive object is required in a significant fraction of systems.

### 3.1 Accelerations predicted for a distribution of companion masses and periods

We now consider Monte Carlo simulations for systems with planets and brown dwarfs of different masses and semi-major axes. The semi-major axis and planet mass distribution is assumed to be power law in form and is drawn from a specified range with limits  $a_{min}$ ,  $a_{max}$  and  $M_{p,min}$  and  $M_{p,max}$ . This type of distribution function was used to fit the radial velocity planet search measurements at the Lick and Keck observatories and the Anglo Australian Telescope by Marcy et al. (2008); Cumming et al. (2008). We assume that the probability of a planet with semi-major axis  $a$  and planet mass  $M_p$

$$dP = CM_p^\alpha a^\beta dM_p da de. \quad (6)$$

(Marcy et al. 2008) find that  $\alpha \approx -1.1$  and  $\beta \approx -0.6$ . The exponent  $\beta = -0.6$  is consistent with  $dN/d\log a \propto a^{0.4}$ . Marcy et al. (2008) find a broad eccentricity distribution exterior to  $a = 0.1 \text{ AU}$  with maximum eccentricity  $e = 0.93$ . The coefficient  $C$  is such that  $\sim 10.5\%$  have planets with mass in range 0.3 to  $10 M_J$  and orbital period in range of 2 to 2000 days (Cumming et al. 2008). Cumming et al. (2008) computed the distribution for  $M_p \sin i$  instead of  $M_p$ , however only a small correction is needed as  $\langle \sin i \rangle = \pi/4 = 0.785$  (Cumming et al. 2008, section 3.0).

We now look at the distribution of accelerations for a population of a fixed companion mass but with a distri-

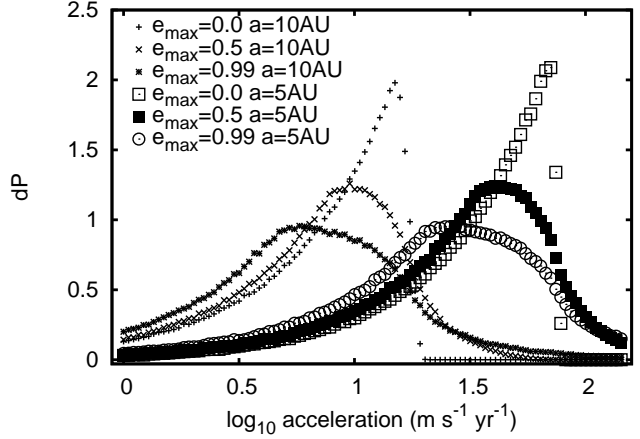


**Figure 1.** Probability distributions for the radial component of acceleration for a population of systems each with a  $10 M_J$  planets at a semi-major axis of 5 AU (large points) and 10 AU (smaller points). The orbital inclinations, mean motions and arguments of perihelia are randomly chosen. Objects are drawn from 3 eccentricity distributions for each planet semi-major axis. The first distribution is for circular orbits, the second with a flat distribution ranging from eccentricity  $e = 0$  to 0.5 and the third ranging from  $e = 0$  to 0.99. Higher eccentricities allow closer approaches and so higher accelerations. A lower mass planet would caused similar curves but shifted to the left because the accelerations would be lower.

bution of semi-major axes. We consider randomly oriented systems populated by  $10 M_J$  planets with semi-major axis chosen from a probability distribution  $dP \propto a^\beta$ , a flat eccentricity distribution ranging from  $e = 0$  to 0.99 and minimum and maximum semi-major axes between  $a_{min}$  and  $a_{max}$ . Figure 2 shows that the probability distribution of the radial acceleration component is only weakly dependent on the exponent of the semi-major axis distribution and on the inner radius of the distribution. These curves would move to the left for a population of lower mass planets as they would cause lower accelerations.

We now consider a planet mass and semi-major axis distribution consistent with equation 6. We begin by normalizing the distribution to be consistent with the fraction of systems,  $\sim 10\%$ , that have planets with mass between 0.3 and  $10 M_J$  and periods between 2 and 2000 days (Cumming et al. 2008). Each systems is assumed to have at most 1 companion. Figure 3 shows the acceleration distributions using this normalization. These probabilities now represent the likelihood of detecting systems with different radial components of acceleration.

In Figure 3 we show 5 probability distributions. The comparison model is the central set of points on Figure 3 with  $\alpha = -1.1$ ,  $\beta = -0.6$  (Marcy et al. 2008). This model has minimum and maximum companion semi-major axes of  $a_{min} = 3 \text{ AU}$ ,  $a_{max} = 100 \text{ AU}$ . As shown from the curve just below the comparison model, the distribution is not sensitive to the minimum semi-major axes. This is likely because the distribution is normalized so that it extends at small semi-major axes to a probability consistent with the number of systems with planets discovered with radial velocity surveys. The comparison model has minimum and maximum planet

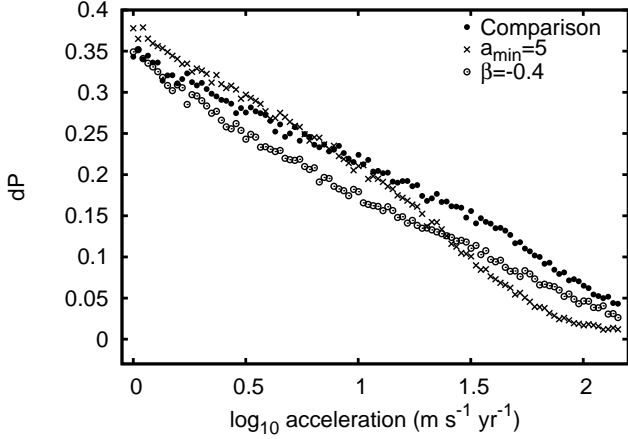


**Figure 2.** Probability distributions for the radial component of acceleration for a population of planets of a given mass but for different semi-major axis distributions. The comparison model, (solid circles) has  $10 M_J$  mass planets chosen with a semi-major axis distribution  $dN \propto a^\beta$  with  $\beta = -0.6$ . The probability for the comparison model is computed assuming that all systems have  $10 M_J$  planets with this distribution and with semi-major axes in the range between  $a_{min} = 3$  AU and  $a_{max} = 100$  AU and eccentricities in the range 0 to 0.99. The probability distribution is not sensitive to  $a_{max}$ . Also shown are distributions for a higher minimum semi-major axis  $a_{min} = 5$  AU and shallower exponent  $\beta = -0.4$  with all other parameters the same as the comparison model. The probability distribution is only weakly sensitive to the inner radius of the distribution and the exponent of the underlying semi-major axis distribution. Power law distributions in the line of sight component of acceleration are predicted.

masses of 0.1 and  $100 M_J$ . The lowest curve shows the effect of truncating the mass distribution to planet masses below  $10 M_J$ . The upper two curves show the effect of changing the exponents  $\alpha$  and  $\beta$ . Shallower mass distributions have a larger number of more massive objects. This leads to a larger number of objects predicted with larger accelerations.

### 3.2 Mass and semi-major axis likelihoods for a given acceleration

For a measured acceleration such as that measured for GL 849 with  $a_r = 4.6 \pm 0.8$  m s<sup>-1</sup> yr<sup>-1</sup> (Butler et al. 2006) we can use our Monte Carlo code to measure the number of systems sampled from a distribution that would be measured with this acceleration. The result of this using the distribution with limits and exponents given in the first line of Table 2 is shown with contours in a plot of  $M_p$  vs  $a$  in Figure 4. Figures 4a and b show contours for an eccentricity distribution with  $e_{max} = 0.99$ , and 0.3, respectively. The highest probability occurs along a line proportional to  $M_p/a^2$  as expected from the scaling in equation 5. Wittenmyer et al. (2006) illustrated upper limits on planet mass as a function of semi-major axis with this scaling. Here we find that the most likely planet mass and semi-major axis mass also have the same scaling. The probability distribution is extremely broad implying that the mass and semi-major axis of the planet cannot be tightly constrained from the probability distribution alone. The distribution is less broad if the eccentricity distribution is truncated. If the eccentricity distri-

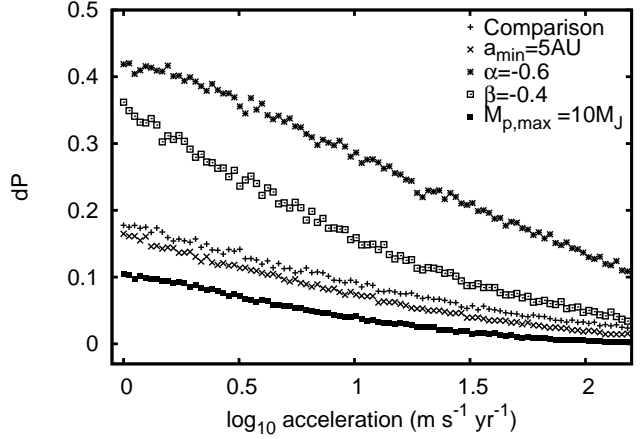


**Figure 3.** Normalized probability distributions for the radial component of acceleration for a population of planets that varies in both mass and semi-major axis. The distributions have been adjusted so that they are consistent with the fraction ( $\sim 10\%$ ) of systems with planets with mass between 0.3 and  $10 M_J$  and periods between 2 and 2000 days (Cumming et al. 2008). Each system is assumed to have at most one companion. The central curve shows the comparison model that has parameters listed in the first line in Table 2. The other curves show probabilities when a single parameter is changed from those of the comparison model. Lowering of the exponent associated with semi-major axis ( $\beta$ ) raises the probability of detecting objects with low accelerations. This is because the distribution is constrained at high velocity accelerations by the radial velocity distributions. Lowering the exponent of the mass distribution ( $\alpha$ ) raises the probability of detecting objects at all accelerations as there are more massive planets. Truncating the planet mass distribution lowers the probability of detecting all accelerations in the range shown here.

bution is broad then 10-100  $M_J$  brown dwarfs between 15-30 AU are somewhat more probable than gas giant planets.

### 3.3 Fractions of objects detected with specific acceleration values

In Table 2 we list the fraction of systems with radial component. of their accelerations above 5, 10 and 25 m s<sup>-1</sup> yr<sup>-1</sup>. Table 2 shows that these fractions are not strongly dependent on the inner semi-major axis of the distribution,  $a_{min}$  so they are not strongly dependent on the time span of the radial velocity survey. The fractions are weakly dependent on the lower planet mass  $M_{p,min}$  and the outer semi-major axis  $a_{max}$  of the distribution. However these fractions are dependent on the outer mass of the distribution and halve if the distribution is truncated at  $10 M_J$  instead at  $100 M_J$ . The exponent,  $\alpha$ , setting the distribution dependence on mass also affects these fractions, with lower exponents predicting a higher fraction of stars with accelerations above a particular value. Lower exponents correspond to a distribution with a larger number of massive objects.

The top part of Table 2 shows distributions normalized and consistent with the known population of extra solar planets within about 5AU. None of the fractions of objects with accelerations above 10 and 25 are predicted high enough to match the fractions 23% and 12% esti-

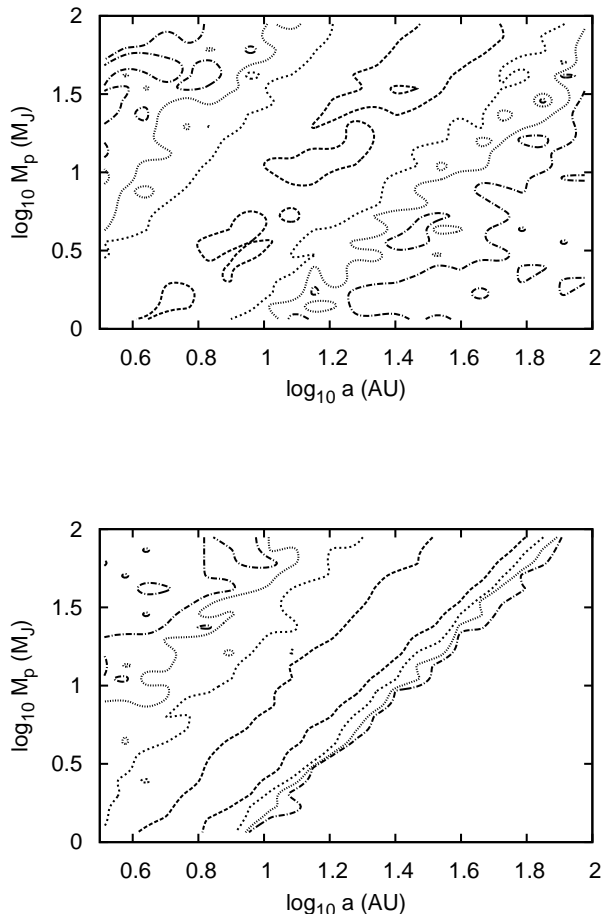


**Figure 4.** Probability contours showing the most likely mass and semi-major axis of a planet that could cause the acceleration  $4.6 \pm 0.8 \text{ m s}^{-1} \text{ yr}^{-1}$  observed for GL 849 (Butler et al. 2006). The contours have been estimated using the planet and semi-major mass distribution and limits listed in the first line of Table 2. Contours are shown with probabilities,  $dP$  in log bins at 0.0003, 0.001, 0.003, and 0.01. Flat eccentricity distributions were assumed. a) For an eccentricity distribution with maximum  $e_{max} = 0.99$ . b) For  $e_{max} = 0.3$ . The probability distribution is broader if the eccentricity distribution is broad. Objects with masses and semi-major axes with  $M_p/a^2 \approx 0.03 M_J/(\text{AU}^2)$  are most likely.

mated from the radial velocity surveys (Cumming et al. 2008; Nidever et al. 2002).

We consider the possibility that the known distribution of companions based on brown dwarf companion imaging surveys could account for the accelerations. In the set of lines shown in Table 2 we show fractions of stars with accelerations above 5, 10 and 25  $\text{m s}^{-1} \text{ yr}^{-1}$  but normalized to a recent companion surveys in a nearby young cluster (Kraus et al. 2008). Kraus et al. (2008) find that 35% of stars have companions in the range 6–435 AU in the mass range  $\sim 10\text{--}500 M_J$ . We assume a stellar companion semi-major axis distribution consistent with a flat distribution in  $\log a$  or an exponent  $\beta = -1$  (Heacox 1999; Kraus et al.

2008). For the companion mass distribution we use a shallower exponent  $\alpha$  in the range  $-0.5$  to  $0$  consistent with the study by Grether & Lineweaver (2006). The bottom part of Table 2 shows that fractions of objects with accelerations above 5, 10 and 25 predicted based on the binary companion distribution are also not high enough to match the observed estimated fractions of 23% and 12% (Cumming et al. 2008; Nidever et al. 2002).

Both normalizing to the population of objects found from radial surveys and from imaging companion surveys predict a deficit of stellar accelerations. To explain the fraction of objects with detected line of sight accelerations an additional population of massive companions in the mass range 10–100  $M_J$  is required. The extrapolation by Cumming et al. (2008) to larger semi-major axis using the mass and semi-major axis distribution suggested that 20% of stars would have gas giant planets within 20 AU. However here we find that this extrapolation is surprisingly conservative and significantly under-predicts the number of stars with observed radial velocity variations.

We ask how many planets would be required to predict the estimated fraction of stars with accelerations above 10 and 25  $\text{m s}^{-1} \text{ yr}^{-1}$ ? The third sets shown in Table 2 show the fractions  $f_{10}$  and  $f_{25}$  predicted for stars assuming that 100% host a companion between 1  $M_J$  and 80  $M_J$  (the highest mass that would be considered a brown dwarf). If we restrict the companion between 4 and 20 AU and use size and period distribution consistent with that estimated by Marcy et al. (2008) then  $f_{10}$  and  $f_{25}$  are predicted to be similar to those estimated from radial velocity surveys. The last line in Table 2 shows the fractions assuming that 3 massive companions are present in 70% of stellar systems. The planet inclinations in each system are assumed to be the same in the Monte Carlo simulation. This possibility too predicts fractions sufficiently high to be similar to those estimated from radial velocity surveys

## 4 SUMMARY AND DISCUSSION

In this paper we have considered the statistics of accelerations that are detected in radial velocity surveys assuming that they are due to massive companions with periods that exceed the time span of the observational survey. We find that the acceleration scales with the planet mass divided by the square of its radius from the host star. The acceleration is independent of the stellar mass. As have previous studies (e.g., Patel et al. 2007), we conclude that detectable accelerations imply that there are gas giants or brown dwarfs in the outskirts (5 to 20 AU semi-major axis range) of their planetary systems.

We have run Monte Carlo simulations to predict the statistics of the line of sight component of the radial stellar acceleration. We find that a distribution of companion masses and semi-major axes causes a probability function for the line of sight component of the stellar acceleration in the form of a constant minus a term proportional to the log of the acceleration.

Given an object with a measured acceleration, Monte Carlo simulations exhibit a maximally likely product of the planet mass divided by its semi-major axis. The distribution is broader if the companion eccentricity distribution is wide.

We find that extrapolation of the planet mass and period distribution found by radial velocity surveys within  $\sim 5$  AU and companion imaging surveys predicts too few systems with detectable accelerations. This suggests that a significant fraction of stars,  $\sim 100\%$ , hosts a gas giant or brown dwarf with semi-major axis between 4 and 20AU. Alternatively 70% of systems could host a few gas giant planets or brown dwarfs in a similar semi-major axis range. A large number of planets in the outer parts of extrasolar systems may not be unexpected if rapid clearing of extra solar systems is required to explain debris disks with central clearings (Faber & Quillen 2007).

We have attempted to match an estimated fraction of stars  $\sim 23\%$  and  $12\%$  with line of sight accelerations component above 5 or 10 and 25  $\text{m s}^{-1} \text{ yr}^{-1}$  estimated from the surveys by Cumming et al. (2008); Nidever et al. (2002). These fractions have not yet been precisely measured or reported. Stars showing a significant fraction of a single period or acceleration variations (as studied by Patel et al. 2007 with full orbital analysis) could be separated from those with constant accelerations. We have not considered the role of jitter and uneven time between observations and other noise sources in affecting the measurements of stellar accelerations. Possible additional information could be learned from combining astrometric and radial velocity information for long period variations. The study here could be refined and broadened to more tightly constrain the population of objects in the outer parts of extrasolar planetary systems. Better understanding of the statistics of accelerations will probably be needed to interpret forthcoming radial velocity surveys of larger numbers of stars.

Support for this work was provided by NASA through an award issued by JPL/Caltech, by NSF grants AST-0406823 & PHY-0552695 and and HST-AR-10972 to the Space Telescope Science Institute. This work is based on observations made with the Spitzer Space Telescope, which is operated by the Jet Propulsion Laboratory, California Institute of Technology under a contract with NASA. We thank Alex Moore, Joss Bland-Hawthorne, Jian Ge and Eric Mamajek for helpful discussions.

## REFERENCES

- Brown, R. A. 2004, *ApJ*, 610, 1079
- Burrows, A. et al. 1997, *ApJ*, 491, 856
- Butler, R. P., Johnson, J. A., Marcy, G. W., Wright, J. T., Vogt, S. S., Fischer, D. A. 2006, *PASP*, 118, 1685
- Cumming, A., Butler R. P., Marcy G. W., Vogt S. S., Wright J. T., Fischer D. A. 2008, *PASP*, 120, 531
- Faber, P., Quillen, A. C. 2007, *MNRAS*, 382, 1823
- Grether, D., Lineweaver, C. H. 2006, *ApJ*, 640, 1051
- Juric, M., Tremaine, S. 2008, *ApJ*, 686, 603
- Heacox, W. D. 1999, *ApJ*, 526, 928
- Hillenbrand, L. A. 2004, in *The Dense Interstellar Medium in Galaxies*, ed. S. Pflanzner et al. (Berlin:Springer), 601
- Kraus, A. L., Ireland, M. J., Martinache, F., Lloyd, J. P. 2008, *ApJ*, 679, 762
- O’Toole, S. J., Tinney, C. G., Jones, H. R. A. Butler, R. P., Marcy, G. W., Carter, B., Bailey, J. 2008, *MNRAS* in press, arXiv:0810.1589
- Patel, S. G., Vogt, S. S., Marcy, G. W., Johnson, J. A., Fischer, D. A., Wright, J. T., Butler, R. P. 2007, *ApJ*, 665, 744
- Marcy, G. W., Butler, R. P., Vogt, S. S., Fischer, D. A., Wright, J. T., Johnson, J. A., Tinney, C. G., Jones, H. R. A., Carter, B. D., Bailey, J., O’Toole, S. J., Upadhyay, S. 2008, *Physica Scripta*, T130, 014001
- Metchev, S., Hillenbrand, L. 2008, *ApJS*, in press, 2008arXiv0808.2982
- Nidever, D. L., Marcy, G. W., Butler, R. P., Fischer, D. A., Vogt, S. S. 2002, *ApJS*, 141, 503
- Wittenmyer, R. A., Endl, M., Cochran, W. D., Hatzes, A. P., Walker, G. A. H., Yang, S. L. S., & Paulson, D. B. 2006, *AJ*, 132, 177
- Wittenmyer, R. A., Endl, M., Cochran, W. D. 2007, *ApJ*, 654, 625
- Wright, J. T., Marcy, G. W., Fischer, D. A., Butler, R. P., Vogt, S. S., Tinney, C. G., Jones, H. R. A., Carter, B. D., Johnson, J. A., McCarthy, C., Apps, K. 2007, *ApJ*, 657, 533

**Table 1.** Fraction of single planet mass and semi-major axis systems that would be seen with accelerations above 5, 10 and 25  $\text{m s}^{-1} \text{ yr}^{-1}$

$M_p(M_J)$	$a(\text{AU})$	$e_{max}$	$f_5$	$f_{10}$	$f_{25}$
10	10	0.0	0.36	0.22	0.00
10	10	0.5	0.34	0.18	0.02
10	10	0.99	0.29	0.15	0.03
10	5	0.0	0.47	0.44	0.34
10	5	0.5	0.46	0.43	0.32
10	5	0.99	0.45	0.40	0.26
5	5	0.5	0.42	0.35	0.14
5	5	0.99	0.40	0.30	0.12
1	5	0.5	0.15	0.02	0.00
1	5	0.99	0.13	0.04	0.01

The fractions  $f_5$ ,  $f_{10}$  and  $f_{25}$  are the fraction of stars predicted with line of sight accelerations above 5, 10 and 25  $\text{m s}^{-1} \text{ yr}^{-1}$  respectively. These fractions were measured from Monte Carlo simulations that considered a distribution of systems each with 1 planet with planet mass  $M_p$  (in Jupiter masses) (as listed in column 1), semi-major axis  $a$  in AU (as listed in column 2) and with an flat eccentricity distribution in the range 0 to  $e_{max}$  (as listed in column 3). Orbit inclinations and mean anomalies are randomly chosen.

**Table 2.** Fraction of systems with a distribution of planet masses and semi-major axes predicted with accelerations above 5, 10 and 25  $\text{m s}^{-1} \text{ yr}^{-1}$

$\alpha$	$\beta$	$a_{min}$	$a_{max}$	$M_{p,min}$	$M_{p,max}$	$e_{max}$	$f_5$	$f_{10}$	$f_{25}$
Normalized to radial velocity searches									
-1.1	-0.6	3	100	0.1	100	0.99	0.05	0.04	0.02
-1.1	-0.6	3	250	0.1	100	0.99	0.05	0.04	0.02
-1.1	-0.6	5	100	0.1	100	0.99	0.04	0.03	0.01
-0.6	-0.6	3	100	0.1	100	0.99	0.19	0.14	0.09
-1.1	-0.4	3	100	0.1	100	0.99	0.09	0.06	0.04
-1.1	-0.6	3	100	0.1	10	0.99	0.02	0.01	0.00
-1.1	-0.6	3	100	0.1	100	0.3	0.06	0.04	0.02
Normalized to an imaging search for companions									
-0.5	-1.0	3	250	0.1	500	0.99	0.08	0.07	0.06
-0.5	-1.0	3	250	0.1	500	0.5	0.09	0.08	0.06
0.0	-1.0	3	250	0.1	500	0.99	0.07	0.06	0.05
0.0	-1.0	3	250	0.1	500	0.5	0.07	0.06	0.05
Assuming 100% of stars have one massive planet or brown dwarf between 4 and 20 AU									
-1.1	-0.6	4	20	1	80	0.3	0.26	0.19	0.10
Assuming 70% of stars have 3 massive planets or brown dwarfs between 4 and 30 AU									
-1.1	-0.6	4	30	1	80	0.3	0.26	0.21	0.14

The fractions  $f_5$ ,  $f_{10}$  and  $f_{25}$  are the fraction of stars predicted with line of sight accelerations above 5, 10 and 25  $\text{m s}^{-1} \text{ yr}^{-1}$  respectively. The exponents  $\alpha$  and  $\beta$  correspond to a companion distribution  $dN \propto M_p^\alpha a^\beta dM_p da de$ . Minimum and maximum distribution semi-major axes  $a_{min}$  and  $a_{max}$  are in AU. Minimum and maximum distribution planet or brown dwarf mass ratios are  $M_{p,min}$  and  $M_{p,max}$  in Jupiter masses. The eccentricity distribution is assumed to be flat with minimum and maximum  $e_{min} = 0$  and  $e_{max}$ .

The top set has distributions normalized so that the number of systems with masses between 0.3 and 10  $M_J$  and periods between 2 and 2000 days is consistent with the 10.5% estimated by Cumming et al. (2008). The second set has distributions normalized so that 35% percent have companions in the mass range  $\sim 12$  to 500  $M_J$  (Kraus et al. 2008). and with semi-major axis in the range 10–430 AU (Kraus et al. 2008). The exponent  $\beta$  for this set is chosen from the approximately flat distribution in  $\log a$  (Heacox 1999; Kraus et al. 2008). The mass exponent  $\alpha$  is chosen to be in the range consistent with that found by Grether & Lineweaver (2006). For the top 2 sets of distributions we assume that each system has at most 1 companion. The third set of simulations is computed assuming that all systems have exactly one massive planet or brown dwarf with semi-major axis between 4 and 20 AU. Exponents  $\alpha$  and  $\beta$  are those estimated by Marcy et al. (2008). For the last set we assume that that 70% of systems have 3 giant planets or brown dwarfs in the region between 4 and 30 AU.